

# Learning Keypoints for Robotic Cloth Manipulation using Synthetic Data

Thomas Lips<sup>1</sup>, Victor-Louis De Gussemé<sup>1</sup> and Francis wyffels<sup>1</sup>

**Abstract**—Assistive robots should be able to wash, fold or iron clothes. However, due to the variety, deformability and self-occlusions of clothes, creating robot systems for cloth manipulation is challenging. Synthetic data is a promising direction to improve generalization, but the sim-to-real gap limits its effectiveness. To advance the use of synthetic data for cloth manipulation tasks such as robotic folding, we present a synthetic data pipeline to train keypoint detectors for almost-flattened cloth items. To evaluate its performance, we have also collected a real-world dataset.

We train detectors for both T-shirts, towels and shorts and obtain an average precision of 64% and an average keypoint distance of 18 pixels. Fine-tuning on real-world data improves performance to 74% mAP and an average distance of only 9 pixels. Furthermore, we describe failure modes of the keypoint detectors and compare different approaches to obtain cloth meshes and materials. We also quantify the remaining sim-to-real gap and argue that further improvements to the fidelity of cloth assets will be required to further reduce this gap. The code, dataset and trained models are available [here](#).

**Index Terms**—Deep Learning for Visual Perception, Simulation and Animation, Data Sets for Robotic Vision

## I. INTRODUCTION

Clothes are everywhere in our living environments. Therefore assistive robots should be able to interact with cloth items and perform tasks such as washing, folding or ironing. However, due to their variety in shape and appearance, complex deformations and self-occlusions, cloth manipulation and perception are challenging [1], [2]. Progress has been made in recent years thanks to the continued integration of data-driven techniques [3]–[5] and the development of new hardware [6], but we do not yet have robots that can reliably flatten, fold or iron arbitrary pieces of cloth.

Part of the reason is that we lack the required amount of data to make these systems generalize. The use of synthetic data has proven an effective direction to overcome this data limit in various domains of robotics [7]–[9] and beyond [10]. Synthetic data can provide arbitrary amounts of perfectly annotated data, but the main concern is to bridge the gap between synthetic and real data, as perfectly covering the real data distribution is often infeasible. Various approaches have been explored to overcome this [7], [8], [10], [11], yet a great deal of engineering effort is usually involved in making sim-to-real work.

In this paper, we want to enable generic robot folding. To this end, we generate synthetic data to learn keypoints on various cloth items after they have been unfolded by



Fig. 1. In this work we learn to detect semantic keypoints on *almost-flattened* clothes in everyday environments. To tackle the large diversity in cloth states, cloth materials and environments, we generate synthetic data to train these keypoint detectors.

a robot. Current unfolding systems are not perfect yet [3], [5], [6] and we therefore detect keypoints on both flattened and slightly deformed clothes. We refer to these cloth states as *almost-flattened*. We detect non-occluded keypoints on clothes of various categories from an RGB image. Using these keypoints, tasks such as folding flattened clothes can be achieved with scripted motions [5], [12], [13]. Several prior works use synthetic data for cloth manipulation [5], [14], [15] but to the best of our knowledge, none have tackled this specific setting. Furthermore, we are also the first to compare the performance of different procedures to obtain cloth meshes and materials.

We generate synthetic data for T-shirts, towels and shorts. This process has three stages: We first procedurally create cloth meshes. In the second stage, these meshes are dropped and deformed to mimic the output of current robotic unfolding systems, using Nvidia Flex [16]. Finally, we render images of the clothes and generate the corresponding annotations. To provide real-world training data and to thoroughly evaluate the performance of the keypoint detectors, we have also gathered a dataset of almost 2,000 images.

We find that keypoint detectors trained on our synthetic data have a mean average precision of 64.3 % on our evaluation dataset, which is an improvement over the baseline trained only on real data. Fine-tuning using real data further improves performance to 74.2%. These results show that our synthetic data pipeline can be used to build state estimators for robotic cloth folding systems. Additionally, we compare several different procedures to generate cloth meshes and materials where we find that the best results are obtained by using random materials and single-layer cloth meshes, even though this decreases fidelity. Finally, we quantify the

<sup>1</sup>AI and Robotics Lab, Ghent University - imec  
Technologiepark 126, 9052 Zwijnaarde, Belgium  
corresponding author: Thomas.Lips@UGent.be

remaining sim-to-real gap and argue that this gap can only be closed by further advancements in cloth asset generation and simulation.

To summarize, our contributions are as follows:

- We build a synthetic data pipeline and use it to train keypoint detectors that enable cloth folding.
- We compare different procedures to obtain cloth meshes and materials, to gain more insight into synthetic data generation for cloth manipulation.
- We provide a real-world dataset of 2,000 images and corresponding annotations of almost-flatted clothes in everyday environments.

## II. RELATED WORK

### A. Robotic Cloth Manipulation

Robotic cloth manipulation has been extensively studied [1], [3], [4], [12], [13], [17]. Most works in robotic laundering focus on unfolding (also called flattening) and folding. Despite the considerable success demonstrated by unfolding pipelines [4]–[6], they frequently yield clothes that aren’t perfectly flattened and have yet to fully demonstrate the desired generalization across various cloth instances and environments

Given flattened clothes, tasks such as folding can be tackled using an appropriate representation and a scripted policy [5], [13]. Several methods have been explored to create such state representations for clothes, including template fitting [4], [12], edge detection [18] and semantic keypoint detection [5], [14], [19], [20]. Many of these works use depth images [14], [18], [20], as these only represent geometry and are not influenced by irrelevant environment elements such as lighting. However, depth images also discard useful information (such as color patterns, seams..) and can lack the required precision [18]. To avoid these limitations, we use RGB images in this work.

In this work, we detect keypoints of almost-flattened clothes that are lying on a surface. By doing so, we aim to facilitate the creation of cloth manipulation systems that operate on the output of an unfolding system and can generalize to arbitrary clothes and environments.

### B. Synthetic data for Robotic Cloth Manipulation

Synthetic data has been used extensively in robotic cloth manipulation research to learn representations and end-to-end policies [5], [14], [15], [19], [21]. A variety of cloth simulators have been used, including Pybullet [22], Nvidia Flex [16] and Blender [23].

As always when learning from synthetic data, obtaining appropriate 3D assets is a key challenge. Many works use a limited number of pre-made cloth meshes which they manually annotate if needed [5], [14], [24]. Others generate single-layer meshes procedurally [19], [21]. The authors of [25] have focused on generating a large dataset of cloth meshes, which is used in [3], [5], though these meshes do not come with annotations of semantic locations or edges.

In this work, we further explore the use of synthetic data for keypoint detection. Our goal is to create a pipeline from

TABLE I

THE ARTF CLOTHES DATASET IN NUMBERS. BOTH SCENES AND CLOTH ITEMS ARE DISTINCT FOR THE TRAIN AND TEST SPLITS TO MEASURE THE GENERALIZATION PERFORMANCE OF TRAINED MODELS.

Cloth Category	# scenes		# cloth items		# Images	
	Train	Test	Train	Test	Train	Test
Towels	6	8	15	20	210	400
T-shirts	6	8	15	20	210	400
Shorts	6	8	8	9	112	180
Boxershorts	6	8	11	11	154	220
Total	6	8	49	60	686	1200

which models can be trained that generalize to arbitrary clothes, deformations and environments.

## III. ALMOST-READY-TO-FOLD CLOTHES DATASET

To train and evaluate the keypoint detectors, we have created a dataset of almost-flattened clothes in which we mimic the output of current robotic unfolding systems [3], [5], [6] by applying small deformations to the clothes. We refer to this dataset as the aRTF Clothes dataset, for almost-ready-to-fold clothes. There have already been some efforts to collect datasets for robotic cloth manipulation [4], [26], [27], but to the best of our knowledge, this dataset is the first to provide annotated real-world of almost-flattened cloth items in household settings.

In the next sections, we briefly describe the data capturing and labeling procedure.

### A. Dataset Capturing

We collected data in 14 distinct household scenes. The cloth items were provided by lab members, though we included towels from the household cloth dataset [28].

For each image, we started by laying the cloth item on the folding surface and then randomly applied some deformations. The deformations include a random pinch to create wrinkles, or folding a side or corner of the cloth upwards or downwards and were determined by listing failure modes of state-of-the-art unfolding pipelines [4]–[6].

We collected the images using a ZED2i RGB-D camera and a smartphone. The camera was positioned to mimic an ego-centric perspective at a distance between 0.5 and 1 m.

The dataset contains a total of 1,896 images and is summarized in Table I. Collecting these images took 2 persons about 15 hours. Fig. 1 shows some examples from the dataset.

### B. Annotating

For each cloth category, we defined a number of semantic locations (keypoints) and annotated these on each image. We use the same semantic locations as Miller et al. [29], except for a single semantic location in the neck opening of T-shirts that we have not used in our work. The semantic locations can be seen in the examples in Fig. 1.

We also labeled the segmentation mask and bounding boxes and use Segment Anything (SAM) [30] for pre-labeling the masks. In total, this labeling effort took a single person about 3 days.



Fig. 2. Examples of the generated synthetic images. Though these single-layer meshes with random materials look unrealistic, they have the best performance out of all evaluated procedures.

#### IV. PROCEDURAL DATA GENERATION PIPELINE

In this section, we describe the synthetic data pipeline we have created to generate synthetic images of clothes. In general, generating synthetic data entails two steps: obtaining the assets (meshes, materials...) and specifying how these assets should be used to create 3D scenes, from which the desired images and their corresponding annotations can then be generated. Tools such as Blender [23] have enabled the latter step. The main challenge typically lies in gathering or creating the required assets, and this typically comes with a trade-off between realism and diversity. As we are dealing with deformable objects, generating the assets is even more complicated: we need not only to obtain cloth meshes but also to generate the desired distribution of configurations for them, i.e., we need to deform them. The next sections will discuss in more detail how we generate cloth meshes and materials, deform the clothes using Nvidia Flex [16], and use Blender [23] to generate images and the corresponding annotations.

##### A. Obtaining Cloth Assets

1) *Cloth meshes*: The first step is to obtain flat cloth meshes. We generate a series of 2D boundary vertices using a template for each cloth type. These templates are inspired on [29]. We then connect the vertices using bezier curves to create single-layer meshes. These bezier curves are used to create the neck of a T-shirt and to better mimic real cloth items by slightly curving edges. For the same reason, we also round all corners of the single-layer mesh. The parameters of the skeleton, the bezier curves and the rounding radii for all corners are sampled from manually tuned ranges. Finally, the meshes are triangulated such that they have edge lengths of at most 1cm and UV maps are generated. We keep track of the vertices that correspond to each semantic location to automatically label the keypoints later on.

2) *Cloth Materials*: Faithfully reproducing cloth materials for rendering requires both mimicking fabrics and producing realistic color patterns. At the same time, we also need these materials to provide sufficient diversity to enable the generalization of the models trained on the data. This combination tends to be infeasible. We have experimented

with various procedures (see Section VI-B) to generate the cloth materials and have found that using random textures from PolyHaven [31] provides the best results. To increase diversity, we mix these textures with a random color.

##### B. Deforming the Meshes

To generate diverse mesh configurations from the flattened meshes, we deform them using the Nvidia Flex cloth simulator [16], which is also used in several previous works on robotic cloth manipulation [3], [5], [32]. We have also experimented with the Blender cloth simulator [23] and Pybullet [22], but found Nvidia Flex to perform better.

To deform the meshes, we randomize their orientation and drop them on a surface to create wrinkles. Afterwards, we sometimes grasp a point on the cloth and use a circular trajectory to create folds. To create both visible and invisible folds, we sometimes flip the cloth by lifting it entirely, rotating it and dropping it again. This procedure differs from the drop-pick-drop procedure used in [5], [15], as we focus on *almost-flattened* clothes instead of arbitrary crumpled states. The parameters of the procedure have been tuned manually to maximize performance.

To load a mesh into Nvidia Flex, we convert all vertices of the mesh to particles and add both stretch stiffness and bending stiffness constraints using the 1-ring and 2-ring neighbors of each vertex, similar to [5], [32]. Additionally, similar to previous work [3], [5], [14], we randomize various physics parameters, including bending stiffness, stretch stiffness, friction and drag to increase diversity.

##### C. Scene Composition

Using the deformed cloth meshes and the cloth materials described before, the procedure to generate a synthetic image and its annotations is explained below.

We sample an environment texture from PolyHaven [31] to create complex scene lighting. At the same time, we use this texture to create a scene background. Thereafter, a rectangular surface is added to the scene to mimic the folding surface. We sample a material from PolyHaven [31] for this plane and randomize its base color to increase diversity and avoid a bias towards certain colors. We then put a cloth mesh on top of the table and solidify the mesh to add some thickness to the layers. Afterwards, we sample a cloth material and apply it to the mesh. To make the keypoint detectors more robust, we place a number of distractor objects on the surface. We sample the objects from the Google Scanned Objects dataset [33]. Next, we randomize the camera position in a spherical cap around the cloth center and point the camera towards the cloth. At this point we render a single image using Cycles, Blender’s physically based renderer, and create a bounding box, segmentation mask and 2D keypoint annotations. For the keypoints, we use raycasting to determine if the vertex that corresponds to the keypoint is occluded. Inspired by [10] we have tried to make the synthetic labels resemble the human labels in the aRTF dataset, which are not necessarily similar to the ground truth labels. We consider a keypoint as visible if any vertex



TABLE II

PERFORMANCE OF THE KEYPOINT DETECTOR FOR VARIOUS DATA SOURCES. TRAINING ON SYNTHETIC DATA OUTPERFORMS THE BASELINE TRAINED ONLY ON REAL DATA. THE PERFORMANCE IS SIGNIFICANTLY IMPROVED BY TRAINING ON SYNTHETIC DATA AND THEN FINE-TUNING ON REAL DATA.

Cloth Type	mAP <sub>2,4,8</sub> (↑)			AKD(↓)		
	real-to-real	sim-to-real	(sim+real)-to-real	real-to-real	sim-to-real	(sim+real)-to-real
T-shirt	54.4	58.2	69.1	14.2	14.0	8.3
Towel	74.4	83.2	88.6	12.5	13.1	6.8
Shorts	50.7	51.4	64.9	23.6	27.3	11.2
All	59.8	64.3	74.2	16.8	18.1	8.7

in its 2-ring neighborhood is visible in the image, as we empirically observed this to correspond better to our human annotations.

#### D. Dataset Generation

The 3-stage procedure explained in Sections IV-B, IV-B and IV-C is used to generate the desired amount of images for all cloth categories. Creating a mesh template is very fast. Deforming a mesh takes about 6 seconds. Rendering takes about 5 seconds for a 512x256 image on our workstation with an Nvidia RTX 3090, 32GB of RAM and an Intel i7 CPU. More details on the procedural data generation pipeline can be found in the accompanying [codebase](#).

### V. KEYPOINT DETECTION

This section provides more details about the keypoint detectors. We describe the model used to detect keypoints and the metrics we use to quantify the performance of the keypoint detectors. We also describe how we ordered the keypoints in image space to deal with the symmetries of cloth objects.

#### A. Model and Training

We detect the keypoints on the full-resolution images and formulate keypoint detection as regression on 2D heatmaps as in [34]. We convert keypoint coordinates into Gaussian blobs on a 2D probability heatmap, and then use these heatmaps (one for each keypoint category) as target for pixel-wise logistic regression using a binary cross entropy loss. The keypoint model uses a Unet [35] inspired architecture and has  $N$  full-resolution heatmaps as output. The encoder of the Unet is a pretrained MaxViT [36] *nano* model, obtained from the timm library [37]. Keypoints are extracted from the predicted heatmaps by searching for local maxima in a 3x3 pixel grid with a threshold of 0.01 on the probability. Downstream applications can then select the keypoint with the highest probability or use the multi-modal heatmaps to reason more globally over the predictions.

As is common [8], [10], we employ a set of image augmentations during training: random cropping, random Gaussian blurring and noise, and random color, contrast and brightness augmentations.

We train models on synthetic and/or the train split of the aRTF dataset (see Table I). As the synthetic datasets tend to have an order of magnitude more data compared to our aRTF

dataset, we use a different set of hyperparameters for each setting. These were obtained using a random hyperparameter search.

We train each model until convergence and use a subset of the aRTF train split as validation set for this purpose. The performance of each model is tested on the test split of the aRTF dataset, using the checkpoint with the best validation performance.

#### B. Evaluation Metrics

**Mean Average Precision.** In this work we want to enable folding and hence we only detect keypoints that are not occluded, as a robot can only interact with those parts of the cloth. This implies a varying number of detections for each keypoint category. Furthermore our model can predict an arbitrary amount of keypoints, as discussed in Section V. Therefore, we use the Average Precision (AP) as in COCO [38] to measure the performance of our models. For each heatmap channel, we classify all predictions as false or true positives using the L2 distance to the ground truth keypoints with thresholds of 2, 4 and 8 pixels. For the aRTF dataset and our image resolution of 512 by 256 pixels, this corresponds to real-world distances between real and predicted keypoints of at most 1, 2 and 4 cm respectively. We report the mean average precision over all thresholds (mAP<sub>2,4,8</sub>). Note that unlike in COCO’s object-keypoint similarity (OKS), we do not scale the distance according to the object size as we believe that absolute errors are more appropriate for robotic manipulation: it does not matter if a T-shirt is a large or small, if you want to grasp it at a specific location you need the same accuracy for both.

**Average keypoint Distance.** Next to this detection measure, we also employ a distance-based metric to quantify performance as in [14], [20]. More specifically, we report the average keypoint distance (AKS), measured in pixels, between the predicted (if any) keypoint with the highest probability and the non-occluded ground truth keypoints.

#### C. Dealing with symmetry

Clothes have (quasi-) symmetries, which means they can have the same appearance on an image for different configurations (e.g. rotating a white towel on a table by 180 degrees will result in the same image). These symmetries must be handled carefully because the keypoint detector cannot distinguish between them.

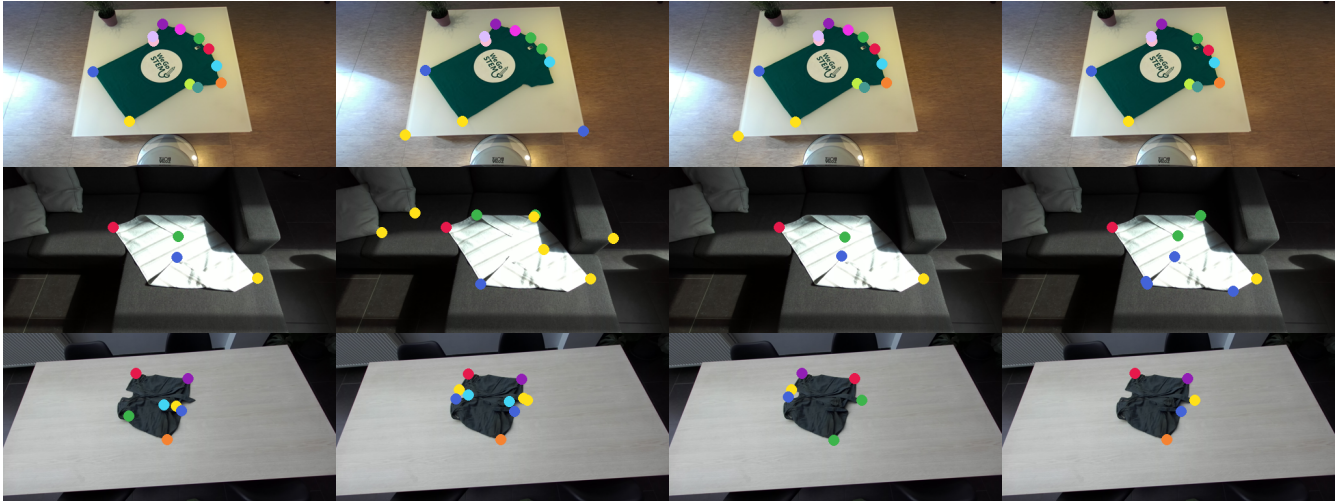


Fig. 3. Illustration of failure modes of the detectors. From left to right, the columns show ground truth keypoints and all predicted keypoints of detectors trained on real data, synthetic data and on both. The first row illustrates how the real baseline produces incomplete and inconsistent keypoints, whereas the second row shows how the detectors still struggle with folds. In the third row, the detectors are confused by an open zipper and mistake it for a leg of the shorts. The keypoint colors encode their category for each cloth type.

One possible solution is to not distinguish between symmetric keypoints by labeling them identically [19], but this results in some loss of information: we can no longer infer the connectivity of the keypoints, which is useful if you want to e.g. grasp the two corners of an edge. Other solutions include using a loss function that is invariant across all symmetries [14], or selecting an arbitrary ordering in the image [5], [24]. A thorough evaluation of these approaches would be out of scope and in this work we have applied an ordering to the keypoints to deal with symmetry. To do so, we have adapted the labels of the synthetic data and the aRTF dataset as follows:

For towels, we have taken the keypoint closest to the top left corner of the bounding box to be the first and its physically adjacent corner that is closest to the top right corner of the bounding box as the second keypoint. The others follow from this convention.

T-shirts or shorts have no rigid motions symmetries. However, detecting the front/back side can be very ambiguous, even on real data, and therefore we treat this as a rotational symmetry. For T-shirts we take as *left* side, the side of which the waist keypoint is closest to the bottom left corner of the T-shirt’s bounding box. For shorts, we use the top left corner of the bounding box.

## VI. EXPERIMENTS

In this section, we train several keypoint detectors on different data sources. We evaluate the performance of all models on the test split of the aRTF dataset (see Table I) using the mean Average Precision (mAP) as metric. In Section VI-A we show that training on the synthetic data (sim-to-real) for three cloth categories results in better performance than training on the aRTF train split (real-to-real), and how fine-tuning on the real data (sim+real-to-real) improves performance significantly. The cloth mesh procedure and

TABLE III  
REALITY GAP OF THE SYNTHETIC DATA AS MEASURED BY THE DIFFERENCE BETWEEN SIM-TO-SIM AND SIM-TO-REAL PERFORMANCE.

cloth type	mAP <sub>2,4,8</sub> (↑)		AKD (↓)	
	sim-to-real	sim-to-sim	sim-to-real	sim-to-sim
T-shirt	58.2	81.8	14.0	5.8
Towel	83.2	84.7	13.1	7.4
Shorts	51.4	79.8	27.3	7.4
All	64.3	82.1	18.1	6.8

cloth materials described in Section IV are compared against other alternatives in Sections VI-B and VI-C.

### A. Main Results

We have trained keypoint detectors for both T-shirts, shorts and towels. For each cloth type, we trained three models using different data sources: the corresponding train split of the aRTF dataset (which we use as a baseline), a dataset of synthetic images and a combination of both by fine-tuning on the aRTF data after training on the synthetic data. We use 10,000 synthetic images per category as we have observed that surpassing this amount does not lead to a significant improvement.

The performance of all models, as measured on the aRTF test splits, is given in Table II. Over all cloth types, the baseline model that is only trained on real data obtains an mAP<sub>2,4,8</sub> of 59.8 and an AKD of 16.8 pixels. Training on synthetic data results in an improved mAP<sub>2,4,8</sub> (64.3) but a lower AKD of 18.1 pixels, caused by a longer tail of the keypoint distances for the model trained on synthetic data. Fine-tuning on the aRTF data results in an mAP<sub>2,4,8</sub> of 74.2 and an AKD of only 8.7 pixels, almost halving the average distance compared to training on real or synthetic data only. When comparing between categories the performance is best

for the towels on both metrics. A few examples of the output of the models trained on a combination of the aRTF train split and synthetic data can be found in Fig. 1. We have also added a [video](#) to the repository where we visualize the keypoint predictions while interacting with various clothes. Using the keypoint detectors, folding policies can be scripted [5], [13]. We demonstrate this by folding T-shirts using scripted motions based on the detected keypoints. We do not report quantitative results, for which our experimenter was not extensive enough, but have included a [video](#) in the project repository.

The above results clearly show the added value of the synthetic data. At the same time, Table II shows that the detectors are not perfect. To provide more insight into the failures of the detectors, we show the predicted keypoints of the models trained on each data source on a number of samples from the aRTF test split in Fig. 3. Each example illustrates a common failure mode: The first row illustrates how training only on the aRTF train split results in models that confuse semantic locations and return many false positives, which is also visible in the second example. The keypoint detectors still struggle with folds, as can be seen in the second example. Despite many efforts to tailor the distribution of mesh deformations in the synthetic data (see Section IV-B), we have not managed to completely solve this problem. The final example in Fig. 3 illustrates how all models have difficulties with a particular configuration of a short in which the opened zipper is confused for a leg. Similar confusions occur for T-shirts as well.

The lack of further improvement when adding more synthetic data and the performance improvement when fine-tuning on the aRTF data already suggest that there is a reality gap for the synthetic data. To measure this, we have evaluated both the sim-to-sim performance and the sim-to-real performance of the models trained on synthetic data. These results can be found in table III. Across all categories, the difference is about 20pp for the mAP and 11 pixels for the AKD, which confirms there is still a substantial reality gap.

### B. Comparing procedures for obtaining cloth meshes

In this experiment, we motivate the use of single-layer meshes for synthetic data generation by comparing three different procedures to generate T-shirt meshes:

- 1) Inspired by [5] we have taken 5 T-shirt meshes from the Cloth3D dataset [25]. We have triangulated the meshes and cleaned up their UV maps. Using Nvidia Flex, we generated a flattened version of these meshes, by dropping them from a certain height. We then manually labeled all keypoints by selecting the corresponding vertices on the mesh. Similar to [14], we have created 10 variants of each mesh by rescaling it, leading to a total of 50 different meshes. Using these meshes, we generate deformed configurations with the procedure discussed in Section IV-B.
- 2) We procedurally generate single-layer T-shirt meshes using a 2D template as described in Section IV-A.1.



Fig. 4. Examples of the considered cloth mesh procedures. Left to right: undeformed single-layer mesh, Cloth3d mesh, single-layer mesh. Though less realistic, using the single-layer meshes results in the best performance.

TABLE IV

COMPARISON OF DIFFERENT PROCEDURES TO OBTAIN CLOTH MESHES. THE SINGLE-LAYER PROCEDURE RESULTS IN THE BEST PERFORMANCE.

Cloth Mesh Procedure	mAP <sub>2,4,8</sub> (↑)	AKD(↓)
Cloth3D subset	43.4	20.6
single-layer	<b>54.3</b>	<b>15.3</b>
single-layer undeformed	53.8	17.9

We then create deformations using the same procedure as above. As these meshes and their annotations are generated procedurally, we can generate arbitrary amounts of meshes, unlike for the cloth3d procedure.

- 3) We use the same 2D templates as above but do not deform them, which results in perfectly flat meshes, similarly to [19].

An example of each mesh procedure can be found in Fig. 4. For each procedure, we generate a dataset of 5,000 T-shirt meshes which we then use to generate 5,000 synthetic images using the pipeline described in Section IV-C. The performance on the aRTF test split of the keypoint detectors trained on these synthetic datasets can be found in table IV. Surprisingly, the more realistic meshes from the Cloth3D dataset perform worse than the less realistic but more diverse single-layer meshes. The undeformed single-layer meshes also perform surprisingly well. Based on these results, we use the single-layer mesh procedure in this paper.

### C. Comparing different cloth materials

In this experiment, we compare different cloth material configurations for rendering:

- 1) For the first configuration, we simply add random materials from PolyHaven [31] to the cloth and mix the base color map with a random color to create more diversity.
- 2) In the second configuration, we apply a uniform color to the clothes as in [3], [5], [15], [19].
- 3) We also compare against a more tailored procedural material: next to uniform colors, we also add striped color maps. We also add random images to the clothes to mimic logos and prints. Furthermore, we procedurally generate a normal map that mimics fabric materials and generates additional wrinkles, similar to [15], [19].

An example of each material can be found in Fig. 5. We have generated datasets of 5,000 images for these materials, using the procedure from Section IV-C. The performance of the keypoint detectors trained on these datasets can be



Fig. 5. Examples of the cloth different materials that were considered. From left to right: uniform colors, a cloth-tailored procedural material and random PolyHaven [31] textures. Though random materials are less plausible, they result in the best performance.

TABLE V  
COMPARISON OF DIFFERENT CLOTH MATERIALS. ADDING RANDOM MATERIALS TO THE CLOTH MESHES LEADS TO THE HIGHEST PERFORMANCE ON THE ARTF TEST SPLIT.

Cloth Materials	mAP <sub>2,4,8</sub> (↑)	AKD(↓)
PolyHaven random	<b>54.3</b>	<b>15.3</b>
cloth-tailored	49.0	22.1
uniform color	35.1	35.4

found in table V. We observe that uniform color materials result in the lowest performance. This is not surprising as the aRTF dataset contains many non-uniform colored cloth items. It is also consistent with findings in our previous work [19], where we also observed a decreased performance for non-uniform cloth pieces. Perhaps more surprisingly, the random materials perform better than the tailored materials even though the latter look more plausible. We therefore use random materials for all other experiments in this paper.

## VII. DISCUSSION

We have created a synthetic data pipeline for clothes and used it to generate images and corresponding keypoint annotations of cloth items that are *almost* flattened. The improved performance when using this synthetic data to train keypoint detectors clearly shows its benefits. At the same time, we stress that the amount of real-world data of the baseline is limited. Scaling up real-world data collection would improve the results of the baseline. However, due to the huge diversity in cloth meshes, their configurations, cloth materials and environments, we argue that synthetic data will still be needed to obtain models that can generalize to all these aspects.

We have found that performance when training on the synthetic data increased as we traded diversity for fidelity for both cloth meshes and materials. However, we also determined that there is a reality gap that limits the sim-to-real performance. We argue that the current lack of realism in favor of diversity is a local optimum, as we do not expect more randomizations to further improve performance. Further increasing the realism of the data generation pipeline will allow to escape from the observed performance limit.

Improving performance will hence require more accurate cloth meshes that contain fine-grained elements such as seams, zippers, pockets and labels, which are all important cues to determine the semantic locations. To apply materials

realistically, the meshes also need to contain accurate UV maps. Furthermore, the meshes also need to be automatically annotated to reduce engineering effort. Leveraging recent advances in generative text-to-3D models [39] could provide an exciting alternative to manually engineering all the above.

Not only do the assets need to be improved, particle-based simulators such as Nvidia Flex [16] have fundamental limitations. Next to the limited realism of the cloth physics [3], [40], we have also found the inherent intertwining of mesh resolution with cloth thickness and deformation granularity hindering. Simulators such as C-IPC [41] provide improved realism [13], though at the cost of additional computational complexity.

Using generative models for end-to-end data augmentation as in [42] is an alternative to manual engineering of 3D assets and physics simulators, though we have found in some initial experiments that keeping the labels consistent when augmenting real data is a challenge.

Though we firmly believe in the benefits of synthetic data and their use for robotic manipulation, we are not convinced that forcing a model to predict keypoints from a static image of heavily deformed clothes lying on a surface is the best way forward: this might be an artificially hard task. Using more interactive perception as in [12] would allow the system to collect more information. Finally, improvements to the generalization of unfolding systems could also reduce the need to handle deformed pieces in the first place.

## VIII. CONCLUSION

In this work, we have described a pipeline to generate synthetic images of clothes with the goal of improving generalization of robotic cloth manipulation systems. By training keypoint detectors on images generated by this pipeline we have validated its usefulness. The resulting models and the aRTF dataset can be used to enable various tasks such as folding or ironing. Furthermore, the pipeline can be easily adapted to train models for other tasks or cloth types.

We have found that models trained on our data generation pipeline, which prioritizes diversity over fidelity, have a decreased performance when transferred to the real world. We argue that future work should focus on increasing fidelity to bridge this reality gap.

A limitation of our work is that we assume the cloth type is already known in advance, which cannot be taken for granted in real-world scenarios. We believe our data generation pipeline can be used for learning to classify clothes as well, but consider this to be out of scope.

## ACKNOWLEDGMENTS

The authors wish to thank Maxim Bonnaerens and Peter De Roovere for their valuable feedback. This project is supported by the Research Foundation Flanders (FWO) under Grant numbers 1S56022N (TL) and 1SD4421N (VDG) and by the euROBIn Project (EU grant number 101070596).



## REFERENCES

- [1] P. Jiménez, “Visual grasp point localization, classification and state recognition in robotic manipulation of cloth: An overview,” *Robotics and Autonomous Systems*, vol. 92, pp. 107–125, 2017.
- [2] H. Yin, A. Varava, and D. Kragic, “Modeling, learning, perception, and control methods for deformable object manipulation,” *Science Robotics*, vol. 6, no. 54, p. eabd8803, 2021.
- [3] H. Ha and S. Song, “Flingbot: The unreasonable effectiveness of dynamic manipulation for cloth unfolding,” in *Conference on Robot Learning*. PMLR, 2022, pp. 24–33.
- [4] Y. Avigal, L. Berscheid, T. Asfour, T. Kröger, and K. Goldberg, “Speedfolding: Learning efficient bimanual folding of garments,” in *2022 IEEE/RSJ International Conference on Intelligent Robots and Systems (IROS)*. IEEE, 2022, pp. 1–8.
- [5] A. Canberk, C. Chi, H. Ha, B. Burchfiel, E. Cousineau, S. Feng, and S. Song, “Cloth funnels: Canonicalized-alignment for multi-purpose garment manipulation,” in *2023 IEEE International Conference on Robotics and Automation (ICRA)*. IEEE, 2023, pp. 5872–5879.
- [6] R. Proesmans, A. Verleysen, and F. Wyffels, “Unfoldir: Tactile robotic unfolding of cloth,” *IEEE Robotics and Automation Letters*, 2023.
- [7] J. Tobin, R. Fong, A. Ray, J. Schneider, W. Zaremba, and P. Abbeel, “Domain randomization for transferring deep neural networks from simulation to the real world,” in *2017 IEEE/RSJ international conference on intelligent robots and systems (IROS)*. IEEE, 2017, pp. 23–30.
- [8] J. Tremblay, T. To, B. Sundaralingam, Y. Xiang, D. Fox, and S. Birchfield, “Deep object pose estimation for semantic robotic grasping of household objects,” in *Conference on Robot Learning*. PMLR, 2018, pp. 306–316.
- [9] N. Rudin, D. Hoeller, P. Reist, and M. Hutter, “Learning to walk in minutes using massively parallel deep reinforcement learning,” in *Conference on Robot Learning*. PMLR, 2022, pp. 91–100.
- [10] E. Wood, T. Baltrušaitis, C. Hewitt, S. Dziadzio, T. J. Cashman, and J. Shotton, “Fake it till you make it: face analysis in the wild using synthetic data alone,” in *Proceedings of the IEEE/CVF international conference on computer vision*, 2021, pp. 3681–3691.
- [11] J.-Y. Zhu, T. Park, P. Isola, and A. A. Efros, “Unpaired image-to-image translation using cycle-consistent adversarial networks,” in *Proceedings of the IEEE international conference on computer vision*, 2017, pp. 2223–2232.
- [12] A. Doumanoglou, J. Stria, G. Peleka, I. Mariolis, V. Petrik, A. Kargakos, L. Wagner, V. Hlaváč, T.-K. Kim, and S. Malassiotis, “Folding clothes autonomously: A complete pipeline,” *IEEE Transactions on Robotics*, vol. 32, no. 6, pp. 1461–1478, 2016.
- [13] V.-L. De Gussemme and F. Wyffels, “Effective cloth folding trajectories in simulation with only two parameters,” *Frontiers in Neurorobotics*, vol. 16, p. 989702, 2022.
- [14] E. Corona, G. Alenya, A. Gabas, and C. Torras, “Active garment recognition and target grasping point detection using deep learning,” *Pattern Recognition*, vol. 74, pp. 629–641, 2018.
- [15] D. Seita, A. Ganapathi, R. Hoque, M. Hwang, E. Cen, A. K. Tanwani, A. Balakrishna, B. Thananjeyan, J. Ichnowski, N. Jamali, *et al.*, “Deep imitation learning of sequential fabric smoothing from an algorithmic supervisor,” in *2020 IEEE/RSJ International Conference on Intelligent Robots and Systems (IROS)*. IEEE, 2020, pp. 9651–9658.
- [16] “Nvidia flex,” <https://docs.nvidia.com/gameworks/content/gameworkslibrary/physx/flex/index.html>.
- [17] J. Zhu, A. Cherubini, C. Dune, D. Navarro-Alarcon, F. Alambeigi, D. Berenson, F. Ficuciello, K. Harada, J. Kober, X. Li, *et al.*, “Challenges and outlook in robotic manipulation of deformable objects,” *IEEE Robotics & Automation Magazine*, vol. 29, no. 3, pp. 67–77, 2022.
- [18] J. Qian, T. Weng, L. Zhang, B. Okorn, and D. Held, “Cloth region segmentation for robust grasp selection,” in *2020 IEEE/RSJ International Conference on Intelligent Robots and Systems (IROS)*. IEEE, 2020, pp. 9553–9560.
- [19] T. Lips and F. De Gussemme, Victor-Louis wyffels, “Learning keypoints from synthetic data for robotic cloth folding,” *RMDO Workshop ICRA*, 2022.
- [20] D. Seita, N. Jamali, M. Laskey, A. K. Tanwani, R. Berenstein, P. Baskaran, S. Iba, J. Canny, and K. Goldberg, “Deep transfer learning of pick points on fabric for robot bed-making,” in *The International Symposium of Robotics Research*. Springer, 2019, pp. 275–290.
- [21] J. Matas, S. James, and A. J. Davison, “Sim-to-real reinforcement learning for deformable object manipulation,” in *Conference on Robot Learning*. PMLR, 2018, pp. 734–743.
- [22] E. Coumans and Y. Bai, “Pybullet, a python module for physics simulation for games, robotics and machine learning,” <http://pybullet.org>, 2016–2021.
- [23] Blender Online Community, “Blender - a 3d modelling and rendering package,” <http://www.blender.org>, Blender Foundation.
- [24] A. Ganapathi, P. Sundaresan, B. Thananjeyan, A. Balakrishna, D. Seita, J. Grannen, M. Hwang, R. Hoque, J. E. Gonzalez, N. Jamali, *et al.*, “Learning dense visual correspondences in simulation to smooth and fold real fabrics,” in *2021 IEEE International Conference on Robotics and Automation (ICRA)*. IEEE, 2021, pp. 11 515–11 522.
- [25] H. Bertiche, M. Madadi, and S. Escalera, “Cloth3d: clothed 3d humans,” in *European Conference on Computer Vision*. Springer, 2020, pp. 344–359.
- [26] A. Verleysen, M. Biondina, and F. Wyffels, “Video dataset of human demonstrations of folding clothing for robotic folding,” *The International Journal of Robotics Research*, vol. 39, no. 9, pp. 1031–1036, 2020.
- [27] T. Ziegler, J. Butepage, M. C. Welle, A. Varava, T. Novkovic, and D. Kragic, “Fashion landmark detection and category classification for robotics,” in *2020 IEEE International Conference on Autonomous Robot Systems and Competitions (ICARSC)*. IEEE, 2020, pp. 81–88.
- [28] I. Garcia-Camacho, J. Borràs, B. Calli, A. Norton, and G. Alenya, “Household cloth object set: Fostering benchmarking in deformable object manipulation,” *IEEE Robotics and Automation Letters*, vol. 7, no. 3, pp. 5866–5873, 2022.
- [29] S. Miller, M. Fritz, T. Darrell, and P. Abbeel, “Parametrized shape models for clothing,” in *2011 IEEE International Conference on Robotics and Automation*. IEEE, 2011, pp. 4861–4868.
- [30] A. Kirillov, E. Mintun, N. Ravi, H. Mao, C. Rolland, L. Gustafson, T. Xiao, S. Whitehead, A. C. Berg, W.-Y. Lo, *et al.*, “Segment anything,” *arXiv preprint arXiv:2304.02643*, 2023.
- [31] PolyHaven Team, “Polyhaven: The public 3d assets library,” <https://polyhaven.com/>.
- [32] X. Lin, Y. Wang, J. Olkin, and D. Held, “Softgym: Benchmarking deep reinforcement learning for deformable object manipulation,” in *Conference on Robot Learning*. PMLR, 2021, pp. 432–448.
- [33] L. Downs, A. Francis, N. Koenig, B. Kinman, R. Hickman, K. Reymann, T. B. McHugh, and V. Vanhoucke, “Google scanned objects: A high-quality dataset of 3d scanned household items,” in *2022 International Conference on Robotics and Automation (ICRA)*. IEEE, 2022, pp. 2553–2560.
- [34] X. Zhou, D. Wang, and P. Krähenbühl, “Objects as points,” *arXiv preprint arXiv:1904.07850*, 2019.
- [35] O. Ronneberger, P. Fischer, and T. Brox, “U-net: Convolutional networks for biomedical image segmentation,” in *Medical Image Computing and Computer-Assisted Intervention—MICCAI 2015: 18th International Conference, Munich, Germany, October 5-9, 2015, Proceedings, Part III 18*. Springer, 2015, pp. 234–241.
- [36] Z. Tu, H. Talebi, H. Zhang, F. Yang, P. Milanfar, A. Bovik, and Y. Li, “Maxvit: Multi-axis vision transformer,” in *European conference on computer vision*. Springer, 2022, pp. 459–479.
- [37] R. Wightman, “Pytorch image models,” <https://github.com/rwightman/pytorch-image-models>, 2019.
- [38] T.-Y. Lin, M. Maire, S. Belongie, J. Hays, P. Perona, D. Ramanan, P. Dollár, and C. L. Zitnick, “Microsoft coco: Common objects in context,” in *Computer Vision—ECCV 2014: 13th European Conference, Zurich, Switzerland, September 6-12, 2014, Proceedings, Part V 13*. Springer, 2014, pp. 740–755.
- [39] B. Poole, A. Jain, J. T. Barron, and B. Mildenhall, “Dreamfusion: Text-to-3d using 2d diffusion,” *arXiv preprint arXiv:2209.14988*, 2022.
- [40] D. Blanco-Mulero, O. Barbany, G. Alcan, A. Colomé, C. Torras, and V. Kyrki, “Benchmarking the sim-to-real gap in cloth manipulation,” *arXiv preprint arXiv:2310.09543*, 2023.
- [41] M. Li, D. M. Kaufman, and C. Jiang, “Codimensional incremental potential contact,” *ACM Trans. Graph.*, vol. 40, no. 4, jul 2021.
- [42] T. Yu, T. Xiao, A. Stone, J. Tompson, A. Brohan, S. Wang, J. Singh, C. Tan, J. Peralta, B. Ichter, *et al.*, “Scaling robot learning with semantically imagined experience,” *arXiv preprint arXiv:2302.11550*, 2023.